Interface Reaction Between Electroless Ni–Sn–P Metallization and Lead-Free Sn–3.5Ag Solder with Suppressed Ni$_3$P Formation

YING YANG,[1] J.N. BALARAJU,[2] YIZHONG HUANG,[1] YEE YAN TAY,[1] YIQIANG SHEN,[1] ZVIAD TSAKADZE,[1] and ZHONG CHEN[1,3]

1.—School of Materials Science and Engineering, Nanyang Technological University, Singapore 639798, Singapore. 2.—Surface Engineering Division, CSIR National Aerospace Laboratories, Bangalore 560017, India. 3.—e-mail: aszchen@ntu.edu.sg

The voids formed in the Ni$_3$P layer during reaction between Sn-based solders and electroless Ni–P metallization is an important cause of rapid degradation of solder joint reliability. In this study, to suppress formation of the Ni$_3$P phase, an electrolessly plated Ni–Sn–P alloy (6–7 wt.% P and 19–21 wt.% Sn) was developed to replace Ni–P. The interfacial microstructure of electroless Ni–Sn–P/Sn–3.5Ag solder joints was investigated after reflow and solid-state aging. For comparison, the interfacial reaction in electroless Ni–P/Sn–3.5Ag solder joints under the same reflow and aging conditions was studied. It was found that the Ni–Sn–P metallization is consumed much more slowly than the Ni–P metallization during soldering. After prolonged reaction, no Ni$_3$P or voids are observed under SEM at the Ni–Sn–P/Sn–3.5Ag interface. Two main intermetallic compounds, Ni$_3$Sn$_4$ and Ni$_{13}$Sn$_8$P$_3$, are formed during the soldering reaction. The reason for Ni$_3$P phase suppression and the overall mechanisms of reaction at the Ni–Sn–P/Sn–3.5Ag interface are discussed.

Key words: Electroless Ni–Sn–P, metallization, interfacial reaction, soldering, intermetallic compound, diffusion

INTRODUCTION

Electrolessly plated Ni–P has been widely used as a soldering metallization material for several decades. Accordingly, interfacial reactions between electroless Ni–P and Sn-containing solders, and the implications for long-term reliability, have been widely studied and are well understood.[1–10] During soldering, reaction between Sn and Ni activates transformation of amorphous Ni–P metallization into a layer of crystalline Ni$_3$P containing numerous voids.[11] The mechanism of formation of such voids has also been explained.[1] Because the Ni$_3$P layer has a fine columnar structure,[1,11–13] Ni diffuses rapidly through the layer, leading to the accelerated interfacial reaction. As a result of this rapid reaction, voids nucleate and grow in the Ni$_3$P layer after

prolonged reaction,[1,4–7,13] contributing to the weakened interface and degraded reliability of the solder joint. To slow the interfacial reaction with lead-free solders, it is necessary to avoid formation of the columnar Ni$_3$P layer or to suppress growth of the rapid diffusion path. In previous studies we developed electroless Ni–W–P[14] and Ni–Co–P[15] metallization which substantially slowed the interfacial reaction. During the Ni–W–P/Sn–3.5Ag interfacial reaction, a layer of amorphous (Ni,W)$_3$P was formed which contained no voids, and in the Ni–Co–P/Sn–3.5Ag reaction addition of Co changed the type, composition, and morphology of the intermetallic compounds (IMCs) formed at the interface. This success prompted us to investigate addition of other ternary elements to electroless Ni–P and to investigate the mechanisms of suppression of the rapid reaction with lead-free solders. Because the voids-containing columnar Ni$_3$P layer is the weak link in the diffusion barrier, a plausible

strategy is to suppress formation of the Ni_3P layer altogether by alloy design. According to the Ni–Sn–P phase diagram at 550°C,[16,17] formation of Ni_3P will be avoided when the Sn concentration is greater than ~10 wt.% (~5 at.%) and the P content is approximately 6–7 wt.%. Instead, the composition falls into the region of $(Ni + Ni_3Sn + Ni_{21}P_6Sn_2)$ at 550°C.[16] Private communication with C. Schmetterer, the author of Refs. 16 and 17, revealed that the Ni–Sn–P phase diagram for temperatures below 550°C is not available because of practical difficulties. As a result, no thermodynamic data can be obtained for a solder reflow temperature of approximately 260°C. Nevertheless we hypothesized that if the ternary phase $(Ni_{21}P_6Sn_2)$ is stable at lower temperatures, the three-phase equilibrium $(Ni + Ni_3Sn + Ni_{21}P_6Sn_2)$ could be maintained without the presence of Ni_3P. This principle is true, even if the three phases are not exactly what they are at 550°C.

To test this hypothesis, Ni–P alloy with incorporation of a high Sn content was prepared for soldering reaction with Sn–3.5Ag. Interfacial reaction between Ni–Sn–P and Sn–3.5Ag solder after reflow and prolonged aging was studied. A mechanism for diffusional formation of IMCs at the Ni–Sn–P/Sn–3.5Ag interface was also proposed. For comparison, the interfacial reaction between the same solder and a binary electroless Ni–P metallization under the same reflow and aging conditions was also studied.

EXPERIMENTAL

Cu plates (6 mm thick, 99.98 wt.%) were used as substrate for electroless plating of both Ni–P and Ni–Sn–P. Before plating, the Cu surface was activated by use of a commercial ruthenium-based pre-initiator. Electroless Ni–P plating was conducted in a commercial acidic sodium hypophosphite bath (MacDermid) at pH 5.3 and 88 ± 2°C for 40 min. Electroless Ni–Sn–P plating was performed in an alkaline bath at pH 9.0 and 88 ± 2°C for 30 min. As listed in Table I, the Ni–Sn–P plating bath contains nickel sulfate and sodium stannate as nickel and tin sources, respectively, sodium hypophosphite as reducing agent, and complexing agents and buffering agents.

The electrolessly coated Cu plates were joined by lead-free Sn–3.5Ag solder to form Ni–P/Sn–3.5Ag

Table I. Composition of the plating bath for electroless Ni–Sn–P

Constituents of plating bath	Concentration
$NiSO_4 \cdot 6H_2O$	20 g/L
$SnCl_2 \cdot 2H_2O$	1 g/L
$NaH_2PO_2 \cdot H_2O$	20 g/L
$Na_3C_6H_5O_7 \cdot 2H_2O$	35 g/L
$(NH_4)_2SO_4$	30 g/L
Lactic acid	4 mL/L

and Ni–Sn–P/Sn–3.5Ag solder joints. Before the joining, a thin layer of no-clean paste flux was applied to the top of the plated Cu surface to remove oxides. Commercially obtained Sn–3.5Ag solder wire with flux in the core was used for soldering. The reflow soldering process was conducted in an IR reflow oven (Essemtec RO-06E) with a peak temperature of 260°C for 60 s, followed by solid-state aging at 200°C for up to 200 h.

The surface morphology and the thickness of the Ni–P and Ni–Sn–P coating layers were observed under a scanning electron microscope (SEM), as also were the interfacial microstructures of both types of solder joint after prolonged aging at 200°C. The composition of the as-deposited, the as-reflowed, and the aged samples were analyzed by use of energy-dispersive x-ray (EDX) spectroscopy incorporated into the SEM. For cross-sectional SEM study, samples were cold mounted in epoxy, polished to a 1-μm finish, then etched with 4% hydrochloric acid to reveal the interfacial microstructure. The newly-formed interfacial compound in the Ni–Sn–P/Sn–3.5Ag solder joint was identified by use of transmission electron microscopy (TEM). The TEM sample was prepared by use of the focused ion beam (FIB) technique.

RESULTS

As-Deposited Metallization

The composition of the deposited Ni–P layer was measured by EDX to be 6–7 wt.% P. As shown in Fig. 1a, the surface of the Ni–P layer was formed of smooth nodules of uneven size. The thickness of the Ni–P layer was approximately 14 μm (Fig. 1b). The deposited Ni–Sn–P layer contained 6–7 wt.% P and 19–21 wt.% Sn. It was observed that the surface morphology of the Ni–Sn–P layer was very similar to that of the Ni–P deposit (Fig. 2a). The thickness of the Ni–Sn–P layer was approximately 12.1 μm (Fig. 2b). It was noted that both coatings adhered well to the Cu substrate (Figs. 1b and 2b).

Liquid-State Interfacial Reactions During Reflow

Figure 3a shows the cross-sectional micrograph of the as-reflowed Ni–P/Sn–3.5Ag solder joint. The primary IMC formed at the joint interface was chunky-shaped Ni_3Sn_4, some of which spalled into the bulk solder. Ni_3Sn_4 is formed by reaction of Sn from the solder with Ni from the Ni–P metallization. A dark layer of Ni_3P formed within the top region of the Ni–P metallization, with a few voids present inside. Formation of these voids has been explained elsewhere.[1] A very thin ternary Ni_2SnP layer was also observed to be present between the Ni_3Sn_4 and Ni_3P layers.[6,18]

Chunky-shaped Ni_3Sn_4 was formed in the as-reflowed Ni–Sn–P/Sn–3.5Ag solder joint (Fig. 3b). In contrast with the as-reflowed Ni–P/Sn–3.5Ag

Interface Reaction Between Electroless Ni–Sn–P Metallization and Lead-Free Sn–3.5Ag
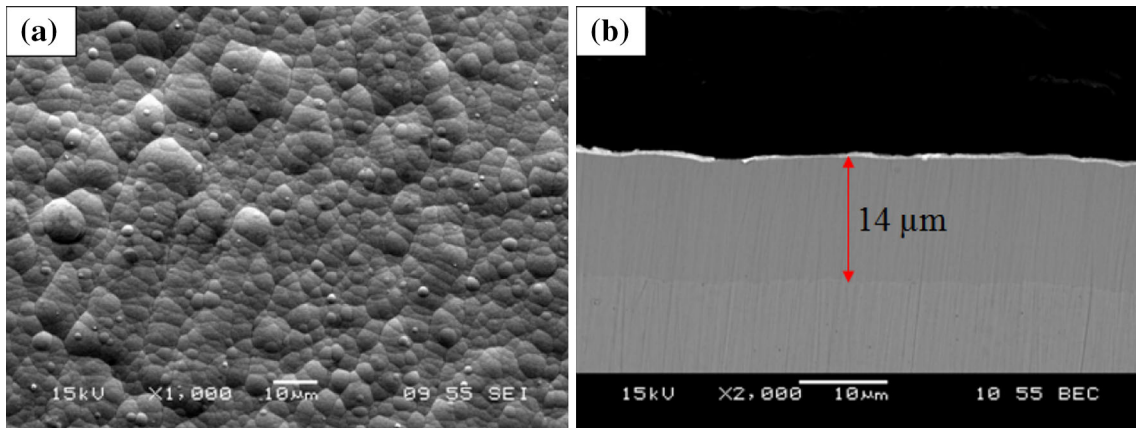Solder with Suppressed Ni_3P Formation

4105

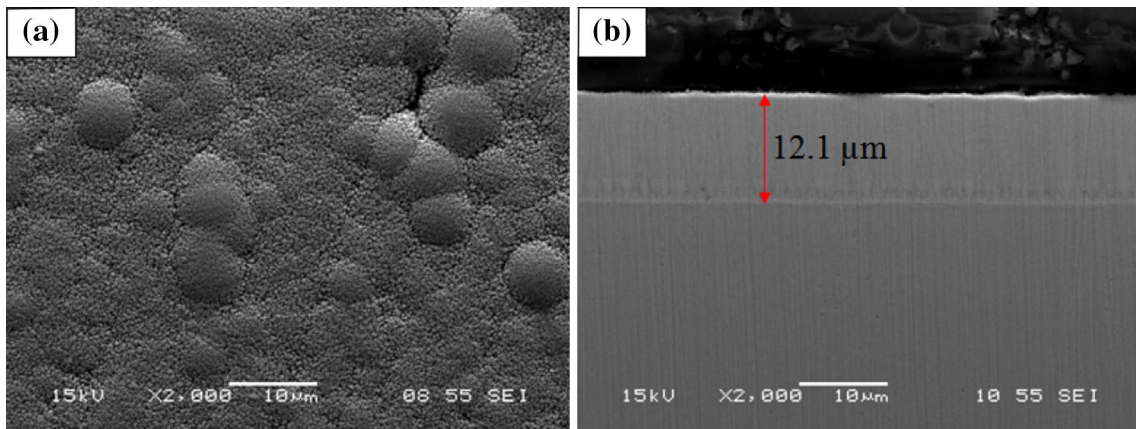Fig. 1. As-deposited Ni–P layer: (a) surface morphology; (b) cross-sectional micrograph.

Fig. 2. As-deposited Ni–Sn–P layer: (a) surface morphology; (b) cross-sectional micrograph.
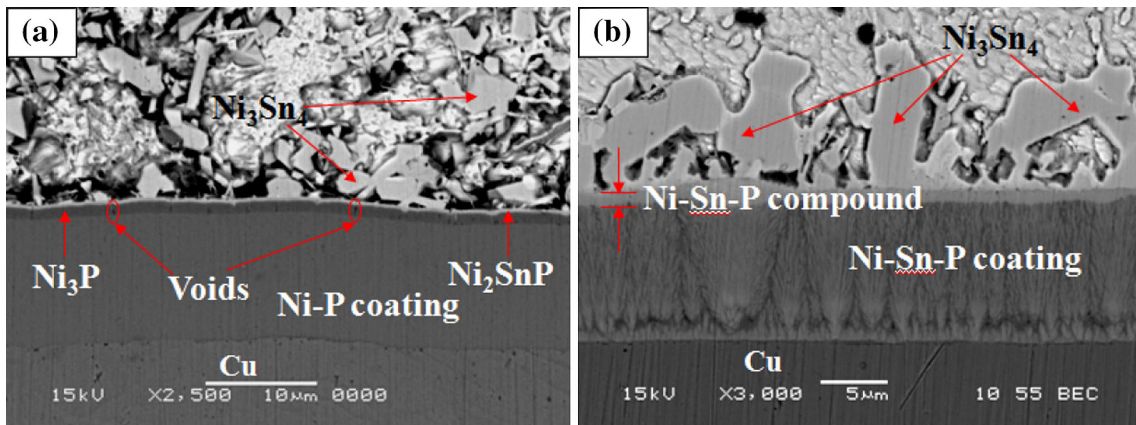

Fig. 3. Back-scattered SEM images showing IMCs formed in the as-reflowed solder joints: (a) Ni–P/Sn–3.5Ag solder joint; (b) Ni–Sn–P/Sn–3.5Ag solder joint.

interface, Ni_3P layer and voids were not formed at the as-reflowed Ni–Sn–P/Sn–3.5Ag interface. This confirms the hypothesis that formation of an Ni_3P layer could be avoided by design of the metallization

composition. It is apparent from Fig. 3b that a thin layer of ternary Ni–Sn–P compound was also observed between the Ni_3Sn_4 layer and the unconsumed Ni–Sn–P metallization. EDX results

indicated that this newly-formed ternary Ni–Sn–P compound contained ~51 at.% Ni, ~34 at.% Sn, and ~15 at.% P. It is a different type of IMC from the Ni_2SnP compound formed at the Ni–P/Sn–3.5Ag interface. Identification of this phase will be discussed below.

It was noticed that the plated Ni–Sn–P layer had clear "tree-like" morphology (Fig. 3b). Within this amorphous layer (to be discussed below), the morphological contrast is because of composition variation, which has also been observed in some cases of electroless Ni–P plating.[19] According to the literature,[19] this compositional variation is caused by periodic fluctuation in the pH of the plating solution adjacent to the deposited surface. It is known that the composition of electrolessly plated Ni–P alloy is very sensitive to solution pH. The pH fluctuation is caused by evolution of hydrogen and reduction of hypophosphite, which reduces the "local" pH. It takes some time for the solution at the "local" metal/solution interface to recover the composition of the bulk solution by diffusion. Therefore such localized depletion/replenish cycles typically lead to lamellar-type morphology in Ni–P plating.[19] In our work, the Ni–Sn–P layer has a columnar growth pattern. This growth pattern, coupled with the pH fluctuation during plating, caused the unique "tree-like" morphology in the Ni–Sn–P layer. An EDX line scan (not shown here) indicated that the dark region had a higher P and lower Sn concentration, whereas the Ni concentration was constant throughout the coating thickness. This compositional variation may be harmful to long-term solder joint reliability; future work is needed to homogenize the layer composition by bath formulation and adjustment of plating conditions.

Solid-State Interfacial Reactions During Aging

Figures 4a, b show the growth of different compounds at the Ni–P/Sn–3.5Ag interface after aging at 200°C for 50 h and 200 h, respectively. The Ni_3Sn_4 layer grew much thicker on aging, with accumulation of Ag_3Sn particles inside. After aging for 50 h, the Ni–P metallization was fully consumed and transformed into an Ni_3P layer (Fig. 4a). The thickness of the Ni_3P layer (~7.4 μm) is much less than that of the as-deposited Ni–P layer (~14 μm). Such shrinkage indicates that Ni atoms diffuse from Ni–P to form Ni_3Sn_4 during the soldering reaction. After aging for 200 h, the thickness of the Ni_3P layer (~5.8 μm) was reduced by approximately 20% as compared with that after aging for 50 h (~7.4 μm), and the thickness of the Ni_2SnP layer
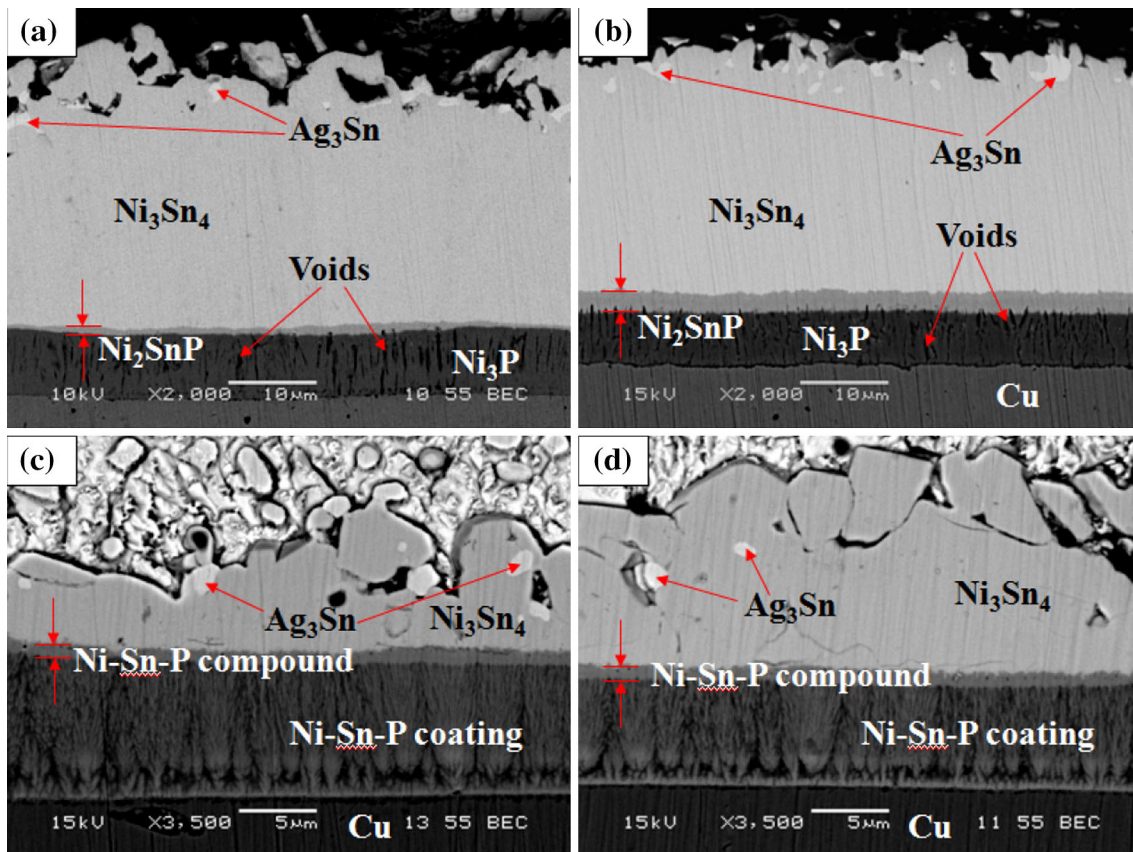

Fig. 4. Back-scattered SEM images showing IMCs formed in the aged solder joints: Ni–P/Sn–3.5Ag solder joint after aging at 200°C for (a) 50 h and (b) 200 h; Ni–Sn–P/Sn–3.5Ag solder joint after aging at 200°C for (c) 50 h and (d) 200 h.

Interface Reaction Between Electroless Ni–Sn–P Metallization and Lead-Free Sn–3.5Ag
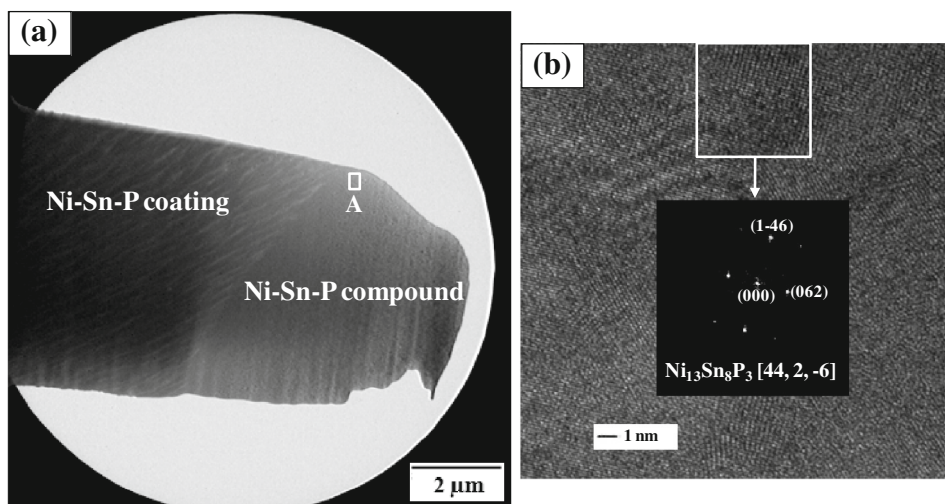Solder with Suppressed Ni₃P Formation

4107

Fig. 5. (a) TEM micrograph showing the Ni–Sn–P/Sn–3.5Ag interface after reflow for 25 cycles, and (b) lattice image and Fourier-reconstructed pattern of region A in (a) with $Ni_{13}Sn_8P_3$.

increased to approximately three times that after aging for 50 h. This indicates that, when the Ni–P layer has been fully consumed, the Ni_2SnP layer grows rapidly at the expense of the Ni_3P layer.[6] There were few voids in the Ni_3P layer of the as-reflowed state (Fig. 3a); however, as the reaction proceeded, with aging, the voids in the Ni_3P layer grew both in size and number (Fig. 4a and b). Interestingly, after the Ni–P metallization was fully consumed (Fig. 4a and b), instead of $(Ni,Cu)_3Sn_4$, only Ni_3Sn_4 formed and no voids were observed at the Cu/Ni_3P interface, indicating that Cu atoms still remained in the substrate even after aging for 200 h.

Figures 4c, d show the growth of different compounds at the Ni–Sn–P/Sn–3.5Ag interface after aging at 200°C for 50 h and 200 h, respectively. Some Ag_3Sn particles were observed to accumulate inside the Ni_3Sn_4 layer. During prolonged aging, the growth of the Ni_3Sn_4 layer at the Ni–Sn–P/Sn–3.5Ag interface was much slower than that at the Ni–P/Sn–3.5Ag interface. After aging for 50 h, approximately 3.3 μm of the Ni–Sn–P metallization was consumed. As a comparison, Ni–P metallization with an original thickness of approximately 14 μm was fully consumed after aging for 50 h (Fig. 4a). Even after aging for 200 h (Fig. 4d), only approximately 5.4 μm Ni–Sn–P metallization was consumed, indicating that the Ni–Sn–P metallization was consumed much more slowly than the Ni–P metallization. The significantly reduced rate of consumption of the Ni–Sn–P metallization is consistent with the much reduced growth rate of the Ni_3Sn_4 layer compared with that at the Ni–P/Sn–3.5Ag interface. It is worth mentioning that no Ni_3P was observed at the Ni–Sn–P/Sn–3.5Ag interface with extended aging for up to 200 h (Fig. 4d), indicating that this phase is thermodynamically avoidable. Moreover, the growth of the Ni–Sn–P

compound at the Ni–Sn–P/Sn–3.5Ag interface was negligible during aging.

Identification of the Newly-Formed Ni–Sn–P IMC

The crystal structure of the newly-formed Ni–Sn–P compound at the Ni–Sn–P/Sn–3.5Ag interface was identified by use of electron diffraction under TEM. The TEM sample was prepared by the FIB technique from the Ni–Sn–P/Sn–3.5Ag interface after reflow for 25 cycles (reflow at 260°C for 60 s as one cycle). Figure 5 shows the TEM micrograph of the FIB sample and the lattice image of the Ni–Sn–P compound. The EDX result for this compound from TEM is consistent with the result obtained from SEM. The lattice image of the Ni–Sn–P compound with the Fourier-reconstructed pattern (Fig. 5b) is matched to $Ni_{13}Sn_8P_3$, combined with the composition result from EDX as secondary evidence, this new compound was identified as $Ni_{13}Sn_8P_3$ with a triclinic lattice ($P1$, $a = 6.456$ Å, $b = 21.291$ Å, $c = 13.247$ Å, $\alpha = 81.052°$, $\beta = 56.260°$, $\gamma = 68.221°$).[20]

DISCUSSION

Only two interfacial compounds, Ni_3Sn_4 and $Ni_{13}Sn_8P_3$ are formed during the Ni–Sn–P/Sn–3.5Ag interfacial reaction. Because the Ni–Sn–P metallization itself contains both Ni and Sn, to determine whether formation of Ni_3Sn_4 is caused by the soldering reaction between Sn from the solder and Ni from the metallization or the reaction between existing Ni and Sn within the metallization at the reflow temperature, XRD was conducted on the as-deposited Ni–Sn–P after annealing at 260°C (the same as the reflow temperature). Figure 6 shows XRD patterns of the Ni–Sn–P deposit before and after annealing at 260°C for 2 h. The XRD spectra were recorded between 2θ from 30° to 80°
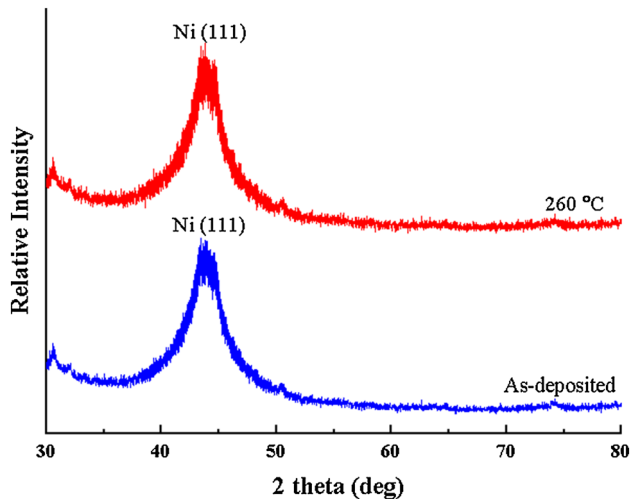
Fig. 6. XRD patterns of the Ni–Sn–P coating before and after annealing at 260°C for 2 h.

with a fixed glancing angle of 2°. It was observed that the pattern for the as-deposited Ni–Sn–P consisted of one broad peak only, with highest intensity belonging to Ni; hence, the as-deposited Ni–Sn–P had an amorphous structure. After annealing at 260°C for 2 h, no peaks from Ni_3Sn_4 were present in the pattern, so the Ni–Sn–P deposit still had an amorphous structure, proving that formation of Ni_3Sn_4 cannot occur by reaction between Sn and Ni present in the Ni–Sn–P metallization itself. Therefore, formation of Ni_3Sn_4 is caused by reaction between Sn atoms diffusing from the solder and Ni atoms from the metallization during soldering between Ni–Sn–P and Sn–3.5Ag. Continuous formation of Ni_3Sn_4 during the soldering reaction leads to the depletion of Ni from the surface of the Ni–Sn–P metallization.

The layer of the compound $Ni_{13}Sn_8P_3$, which has not been reported for any soldering systems, thickens as reaction proceeds. Here we propose a diffusional formation mechanism based on several observations in this work. According to the literature it has been proved there is no out-diffusion of P atoms from the Ni–P metallization during the soldering reaction.[1] In this work, the P atoms in the Ni–Sn–P metallization are also believed to remain in the metallization layer during the soldering reaction. This is probably best confirmed by comparing the compositions of the as-deposited Ni–Sn–P layer (77 at.% Ni, 10 at.% Sn and 13 at.% P) and the newly-formed $Ni_{13}Sn_8P_3$ layer (54 at.% Ni, 33 at.% Sn and 13 at.% P on the basis of the chemical formula). Because both layers have a similar P concentration, it is most likely that the Ni–Sn–P deposit is transformed into $Ni_{13}Sn_8P_3$ during the soldering reaction. As the Ni and Sn concentrations in the two neighboring layers are different, we must explain the diffusion paths for these two elements during the soldering reaction.

Formation of Ni_3Sn_4 causes depletion of Ni from the surface of the Ni–Sn–P layer, so the uppermost region of the Ni–Sn–P layer is transformed into a phase with a lower Ni concentration, in agreement with the fact that $Ni_{13}Sn_8P_3$ has a lower Ni content than the Ni–Sn–P metallization. Because $Ni_{13}Sn_8P_3$ has a higher Sn content than the Ni–Sn–P deposit, it is speculated that transformation of the Ni–Sn–P deposit into the $Ni_{13}Sn_8P_3$ compound requires Sn supply from the solder, which is similar to the formation of Ni_2SnP during the Ni–P/Sn–3.5Ag interfacial reaction.[6,21–24] On the basis of these arguments, we believe that polycrystalline $Ni_{13}Sn_8P_3$ is formed by transformation of amorphous Ni–Sn–P metallization with outward diffusion of Ni and inward diffusion of Sn during the soldering reaction.

To support the proposed diffusional interface reaction mechanism, compositional area mapping was performed on the Ni–Sn–P/Sn–3.5Ag interface after aging at 200°C for 200 h (Fig. 7), it was clearly seen that P atoms remained in the Ni–Sn–P metallization and $Ni_{13}Sn_8P_3$ layers. In contrast, Ni atoms diffused from the Ni–Sn–P layer to form Ni_3Sn_4. Signals from Sn atoms were detected in all the layers except the Cu substrate. This is in agreement with the aforementioned diffusional mechanism of formation of Ni_3Sn_4 and $Ni_{13}Sn_8P_3$ at the Ni–Sn–P/Sn–3.5Ag interface.

Figure 8 schematically illustrates the mechanism of diffusional formation of IMCs at the Ni–Sn–P/Sn–3.5Ag interface. Sn atoms diffusing from the solder react with Ni atoms from the Ni–Sn–P metallization to form Ni_3Sn_4. The uppermost region of the Ni–Sn–P metallization thus becomes Ni-depleted, because of out-diffusion of Ni to form Ni_3Sn_4. Because Sn is the faster diffusant in Ni_3Sn_4,[25] some Sn atoms will also reach the Ni_3Sn_4/Ni–Sn–P interface to form $Ni_{13}Sn_8P_3$. Continued growth of Ni_3Sn_4 requires Ni supply from the Ni–Sn–P layer, so Ni atoms must diffuse through the formed $Ni_{13}Sn_8P_3$ layer to react with Sn atoms from the solder. As further verification, we applied the law of mass conservation at the Ni–Sn–P/Sn–3.5Ag interface to examine evolution of the thickness of the Ni–Sn–P metallization, Ni_3Sn_4, and $Ni_{13}Sn_8P_3$ layers. It was proved that all the Ni atoms which diffuse from the Ni–Sn–P layer participate in the reaction to form Ni_3Sn_4, and depletion of Ni from the surface of the Ni–Sn–P layer leads to formation of the $Ni_{13}Sn_8P_3$ layer (details are omitted in this paper).

Avoidance of the porous columnar Ni_3P layer is the reason for the slower interface reaction in Ni–Sn–P metallization. In Ni–P metallization, the Ni_2SnP IMC layer between the Ni_3Sn_4 IMC and the Ni–P metallization is void-free and could, thus, also be an effective barrier to diffusion. However, the Ni_2SnP layer thickness remains very thin until the Ni–P metallization is fully consumed, after which it grows rapidly by "consuming" the existing Ni_3P layer with inherited voids.[6] Thus, the Ni_2SnP layer has limited action as a diffusion barrier. In Ni–Sn–P metallization, although the $Ni_{13}Sn_8P_3$ layer is also
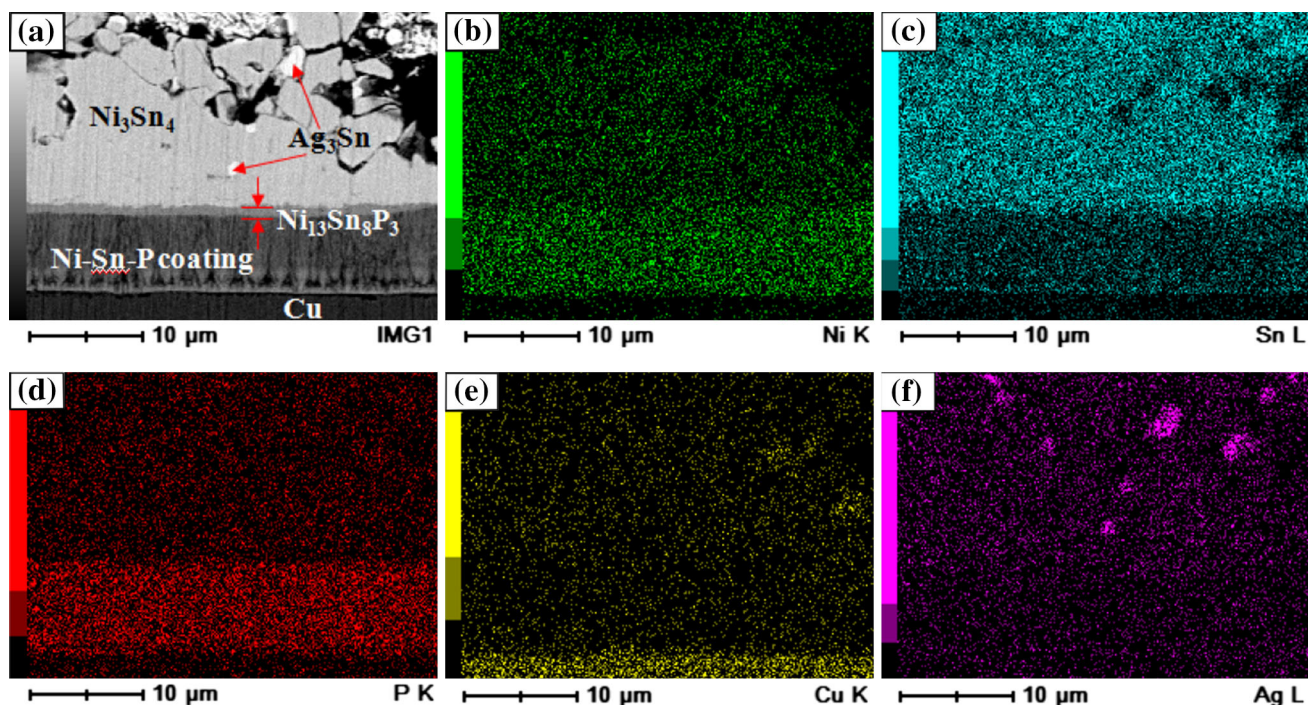
Fig. 7. EDX element mapping analysis of the Ni–Sn–P/Sn–3.5Ag interface after aging at 200°C for 200 h: (a) SEM image, (b) mapping for Ni, (c) mapping for Sn, (d) mapping for P, (e) mapping for Cu, and (f) mapping for Ag. Element concentration decreases with decreasing color intensity.
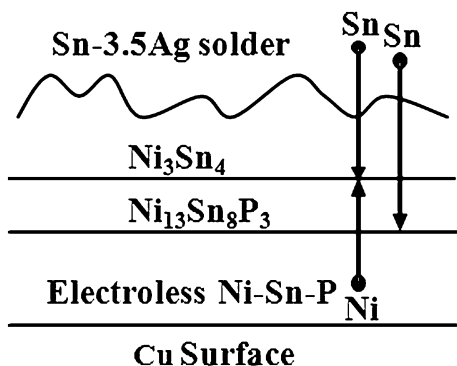

Fig. 8. Schematic illustration of the mechanism of diffusional IMC formation at the Ni–Sn–P/Sn–3.5Ag interface.

thin within the duration of the aging treatment, elimination of the rapidly diffusing Ni_3P layer leads to the large difference in the rate of metallization consumption for Ni–P and Ni–Sn–P. In other words, the good performance of the diffusion barrier in Ni–Sn–P metallization is achieved not by adding a better-performing barrier layer but by eliminating the worst-performing Ni_3P layer.

CONCLUSIONS

In this study, an electrolessly plated Ni–Sn–P alloy (6–7 wt.% P and 19–21 wt.% Sn) has been developed as alternative Ni-based metallization for lead-free soldering. Interfacial reaction between Sn–3.5Ag solder and electroless Ni–Sn–P after reflow and aging was investigated, with the interfacial reaction between the same solder and electroless Ni–P (6–7 wt.% P) under the same reflow and aging conditions as the standard for comparison. Only two IMCs, Ni_3Sn_4 and $Ni_{13}Sn_8P_3$ are formed during the Ni–Sn–P/Sn–3.5Ag interfacial reaction. The Sn atoms from the solder react with the Ni atoms from the Ni–Sn–P metallization to form Ni_3Sn_4, and, as a result, the upper surface of the metallization layer becomes Ni-depleted. The Sn atoms from the solder also diffuse through the formed Ni_3Sn_4 layer to reach the Ni_3Sn_4/Ni–Sn–P interface, and react with the Ni-depleted region of the Ni–Sn–P layer to form the second IMC—$Ni_{13}Sn_8P_3$. This reaction mechanism was proved by study of the mass balance of Ni during Ni–Sn–P/Sn–3.5Ag interfacial reaction, which confirmed that all the Ni atoms diffusing from the Ni–Sn–P layer participated in the reaction to form Ni_3Sn_4. With successful elimination of the rapid diffusion path, i.e. the columnar Ni_3P layer, the Ni–Sn–P metallization was consumed much more slowly than the Ni–P metallization. Therefore, electroless Ni–Sn–P alloy with a high Sn content is a promising metallization material for lead-free soldering.

REFERENCES

1. M. He, Z. Chen, and G.J. Qi, *Acta Mater.* 52, 2047 (2004).

2. M. He, A. Kumar, P.T. Yeo, G.J. Qi, and Z. Chen, *Thin Solid Films* 462–463, 387 (2004).
3. M. He, Z. Chen, G.J. Qi, C.C. Wong, and S.G. Mhaisalkar, *Thin Solid Films* 462–463, 363 (2004).
4. A. Kumar, M. He, and Z. Chen, *Surf. Coat. Technol.* 198, 283 (2005).
5. A. Kumar, Z. Chen, S.G. Mhaisalkar, C.C. Wong, P.S. Teo, and V. Kripesh, *Thin Solid Films* 504, 410 (2006).
6. A. Kumar and Z. Chen, *J. Electron. Mater.* 40, 213 (2011).
7. H.B. Kang, J.H. Bae, J.W. Yoon, S.B. Jung, J. Park, and C.W. Yang, *Scripta Mater.* 64, 597 (2011).
8. M. He, W.H. Lau, G.J. Qi, and Z. Chen, *Thin Solid Films* 462–463, 376 (2004).
9. M. He, Z. Chen, and G.J. Qi, *Metall. Mater. Trans. A* 36, 65 (2005).
10. A.Kumar Mona and Z. Chen, *IEEE Trans. Adv. Pack.* 30, 68 (2007).
11. J.W. Jang, P.G. Kim, K.N. Tu, D.R. Frear, and P. Thompson, *J. Appl. Phys.* 85, 8456 (1999).
12. P.L. Liu, Z.K. Xu, and J.K. Shang, *Metall. Mater. Trans. A* 31, 2857 (2000).
13. K. Zeng and K.N. Tu, *Mater. Sci. Eng. R* 38, 55 (2002).
14. Y. Yang, J.N. Balaraju, S.C. Chong, H. Xu, C. Liu, V.V. Silberschmidt, and Z. Chen, *J. Alloys Compd.* 565, 11 (2013).
15. Y. Yang, J.N. Balaraju, Y.Z. Huang, H. Liu, and Z. Chen, *Acta Mater.* 71, 69 (2014).
16. C. Schmetterer, J. Vizdal, A. Kroupa, A. Kodentsov, and H. Ipser, *J. Electron. Mater.* 38, 2275 (2009).
17. C. Schmetterer and H. Ipser, *Metall. Mater. Trans. A* 41, 43 (2010).
18. Z. Chen, M. He, and G.J. Qi, *J. Electron. Mater.* 33, 1465 (2004).
19. Z. Chen, X. Xu, C.C. Wong, and S. Mhaisalkar, *Surf. Coat. Tech.* 167, 170 (2003).
20. F.J. García-García, A.K. Larsson, and S. Furuseth, *Solid State Sci.* 5, 205 (2003).
21. Y.C. Lin, T.Y. Shih, S.K. Tien, and J.G. Duh, *Scr. Mater.* 56, 49 (2007).
22. Y.C. Lin and J.G. Duh, *Scr. Mater.* 54, 1661 (2006).
23. Y.C. Lin, T.Y. Shih, S.K. Tien, and J.G. Duh, *J. Electron. Mater.* 36, 1469 (2007).
24. Y.C. Lin, K.J. Wang, and J.G. Duh, *J. Electron. Mater.* 39, 283 (2010).
25. C.E. Ho, S.C. Yang, and C.R. Kao, *J. Mater. Sci. Mater. Electron.* 18, 155 (2007).